Non-$2k_F$ charge density wave induced by phonon dispersion in one-dimensional Peierls conductors

1995 J. Phys.: Condens. Matter 7 8287

(http://iopscience.iop.org/0953-8984/7/43/009)

J. Phys.: Condens. Matter 7 (1995) 8287–8315. Printed in the UK

Non-$2k_F$ charge density wave induced by phonon dispersion in one-dimensional Peierls conductors

Jean-Luc Raimbault and Serge Aubry
Laboratoire Léon Brillouin, CEA-CNRS, CE-Saclay, 91191 Gif-sur Yvette Cédex, France

Received 31 May 1995, in final form 27 August 1995

Abstract. Standard Peierls theory predicts that the wave-vector of the charge density wave (CDW) induced by the electron–phonon coupling in the ground-state of a one-dimensional conductor is twice the Fermi wave-vector $2k_F$. At moderately large electron–phonon coupling, beyond the TBA (transition by breaking of analyticity), it is known that this CDW becomes an array of interacting bipolarons. In the simplest models, such as the 1D adiabatic Holstein model, the bipolaron interactions are repulsive and the ground state remains a $2k_F$ CDW of equidistant bipolarons. We show that (apparently) minor changes in the phonon spectrum of the model induce extra elastic forces between the bipolarons, which could break the bipolaronic $2k_F$ CDW ordering.

This effect is studied in detail in the modified 1D Holstein model, where the optical phonon has a non-zero dispersion which is chosen positive in order that an extra force that appears between the bipolarons be attractive. The Coulomb forces between the bipolarons are initially neglected. An accurate numerical study modelled on the standard analysis of multiphase points confirms that, in a large part of the phase diagram, the CDW ground state separates in two phases, which correspond to two CDW with different $2k_F$ wave-vectors (which are generally commensurate) and thus different electronic densities. These separations, into phases called either 'parent' or 'non-parent', are studied on the basis of the Farey construction of rational numbers.

The long-range Coulomb interaction between the charged bipolarons, forbids any macroscopic phase separation in two phases with different electronic densities. The bipolaron structure then has to be a periodic sequence of alternate domains of the two CDW phases on the microscopic scale. The resulting structure is a new CDW with a modulation wave-vector that is not $2k_F$.

We suggest that the aberrant wave-vector observed in the real CDW system $(TaSe_4)_2I$ could be interpreted along the ideas developed in this paper. Although this compound shares many of the usual properties of quasi-one-dimensional conductors with CDW, the component of the modulation wave-vector $0.085c^*$ in the chain direction is, unusually, quite different from the value $2k_F = c^*$ expected from band filling. The CDW in $(TaSe_4)_2I$ could correspond to a non-standard bipolaron ordering due to a strong attractive elastic interaction between the bipolarons along the chain competing with the long-range Coulomb forces.

1. Introduction

According to standard Peierls–Fröhlich theory, the ground-state of a one-dimensional electronic system coupled to phonons is always a charge density wave (CDW) associated with a periodic lattice distortion (PLD) with the same wave-vector which is twice the Fermi wave-vector $2k_F$. It can be either commensurate or incommensurate with the lattice wave-vector according to the band filling [1, 2]. Peierls–Fröhlich theory is basically a theory valid at small electron–phonon coupling.

Some years ago, Noguera and Pouget [9, 11] improved the standard mean field treatment of Peierls–Fröhlich CDW by taking into account the curvature of the energy dispersion

0953-8984/95/438287+29$19.50

curve of the bare electron versus its wave-vector (which yields a finite effective mass for the electron). On this basis they claimed to explain the observed wave-vector variation as a function of temperature in many real CDW and, in particular, in blue bronze. This result can be questioned for technical reasons and, because it contradicts earlier results by Quémerais [10], Noguera and Pouget noted a second possible interesting contribution to the CDW wave-vector variation, which comes from the dispersion of the phonon curve that we are going to consider here. It is the purpose of this paper to prove that this effect may have more drastic physical consequences. The wave-vector of the CDW may no longer be $2k_F$, and the CDW can be broken into different phases with different electronic densities. We only focus on the properties at 0 K of the CDW ground state.

Before describing our results we recall, in section 2, some of our early results which were not predicted by standard Peierls–Fröhlich theory and present, on this basis, the qualitative ideas of the origins of this work. Section 3 describes the modified Holstein model and notations. The single bipolaron and their pair interaction are calculated in section 4. Section 5 describes the many-bipolaron ground state and their phase separations. Finally, in the concluding remarks of section 6, we discuss the role of Coulomb forces and the possible physical consequences of this work. An interpretation of the anomalous value for the observed CDW wave-vector in $(TaSe_4)_2I$ is suggested.

2. Standard ordering for 1D bipolaronic ground states

It has been shown through an accurate numerical analysis that, for the incommensurate CDW, there is a second-order phase transition between a Peierls–Fröhlich CDW and a bipolaronic CDW at a moderately large electron–phonon coupling [3]. This transition, called 'transition by breaking of analyticity' (TBA), corresponds physically to a metal–insulator transition by extinction of the Fröhlich conductivity due to lattice pinning of the CDW. This transition is associated with a gap opening in the phonon spectrum and the system becoming charge defective. In the commensurate case there is no TBA, because the CDW is always pinned to the lattice and thus is insulating at 0 K. A prototype model that exhibits the characteristic features associated with CDW is the 1D adiabatic Holstein model [4]. This model contains only one dimensionless reduced parameter, but the physical features that are found for it extend, for the most part, to more realistic although more complicated CDW models.

This model represents a single electron band with onsite coupling with a dispersionless optical phonon band. It was initially introduced for exhibiting polarons and bipolarons. A single polaron corresponds to a localized electron that is self-trapped in the potential well created by the lattice distortion generated by the electron–phonon coupling. When there is no electron–electron repulsion, it takes less energy for two electrons to form a bipolaron where the two electrons self-localize in the same electronic state but with opposite spins. *A priori*, this concept only looks clear when the electron density is weak enough in order that the electronic states almost do not overlap. In fact, it can be extended at any electronic density, even when the bipolaron wavefunctions overlap.

It has been proven for this model [5, 6] that, when the electron–phonon coupling is large enough, there are infinitely many bipolaronic configurations, most of them being chaotic. More precisely, considering the total energy of the system while the electrons are in their ground state for a given set of onsite lattice distortions $\{u_l\}$, the variational energy which depends on $\{u_l\}$ exhibits infinitely many local minima. Each of these minima can be associated with a set of pseudo-spins $\{\sigma_l\}$ characterizing the spatial distribution of a

bipolaronic configuration ($\sigma_i = 1$ means that a bipolaron is present at site i, and $\sigma_i = 0$ means no bipolaron). Reciprocally, for each set of pseudo-spins $\{\sigma_i\}$, there exists a well defined local minimum of the corresponding bipolaronic configuration. Since the set $\{\sigma_i\}$ is arbitrary, most of these bipolaronic configurations are chaotic.

At large electron–phonon coupling, the ground state of the system is a bipolaronic structure [5], which corresponds to an array of bipolarons with a special ordering superimposed on the lattice, and which is described by a special set of pseudo-spins. This special ordering is *a priori* unknown. However, in the simple 1D Holstein model, this ground state is found numerically to correspond to equidistant bipolarons on the discrete lattice associated with the pseudo-spin configuration [3]:

$$\sigma_i = \chi(i\zeta + \alpha) \tag{1}$$

where $\chi(x)$ is a 1-periodic function defined as

$$\chi(x) = \begin{cases} 1 & 0 \leqslant x < \zeta \quad (2a) \\ 0 & \zeta \leqslant x < 1 \quad (2b) \end{cases}$$

and ζ is the band filling (or density of bipolarons per site); α is an arbitrary phase. The resulting structure turns out to be a bipolaronic CDW with the same wave-vector $2k_F$ as predicted by Peierls–Fröhlich. At the TBA, the size of the bipolarons diverges and the bipolaronic CDW becomes a Peierls–Fröhlich CDW.

The fact that the wave-vector of the bipolaronic CDW in 1D models remains at $2k_F$ is not a universal result. The resulting structure of the bipolarons is determined by the interaction potential between the bipolarons. These interactions can be formally represented at low temperature by a pseudo-spin Hamiltonian $H(\{\sigma_i\})$ which depends on $\{\sigma_i\}$. Although this Hamiltonian contains in principle all possible multi-spin interactions, let us consider only the pair interactions $J(n)\sigma_i\sigma_{i+n}$ between two bipolarons which become the dominant terms at large coupling: $J(n) = J_{el}(n) + J_{ph}(n) + J_{Coul}(n)$ can be split (approximately) into the sum of three components. The first interaction, $J_{el}(n)$, originates from the overlap between the orbitals of two bipolarons. It is repulsive and decays exponentially as a function of their relative distance, n, as well as the electronic wavefunction of a single bipolaron. The second interaction, $J_{ph}(n)$, is mediated by the elastic deformation of the phonon field generated by two polarons. This interaction also decays exponentially as a function of the relative distance, but its sign depends on the details of the phonon dispersion. It may be attractive, repulsive or oscillating as a function of n. The third interaction, $J_{Coul}(n)$, represents the long-range Coulomb forces between the bipolarons which have twice the electronic charge; it is repulsive at all distances. The existence of these interactions between the bipolarons was quoted in an earlier paper by Emin [7] and also suggested by Alexandrov and co-workers [8].

In the original Holstein model there is no phonon dispersion, i.e. the lattice distortion at site i does not interact with the lattice distortion at a different site j and the Coulomb force is not taken into account. It appears that the bipolaron interaction $J(n)$ behaves as $J_{el}(n)$ and is repulsive at all distances. The net result, confirmed by numerical observations, is that the ground state is obtained for equidistant bipolarons, i.e. a $2k_F$ bipolaronic CDW.

In real systems there is generally a phonon dispersion, which can induce non-repulsive forces between the bipolarons. The purpose of this paper is to analyse a simple modified Holstein model with a phonon dispersion. This modified model was already proposed by Holstein as a more realistic model for real molecular systems. For this purpose, we add a

small coupling between the distortions at neighbouring sites which produces an attractive interaction between the bipolarons. Because of this apparently minor change in the model, the $2k_F$ bipolaronic CDW undergoes separation between two phases with different electronic densities when increasing the electron–phonon coupling beyond relatively small values. This situation contrasts with those numerically observed in the Falicov–Kimball model [34], where phase separations between phases with different electric charges are found at small coupling while the periodic $2k_F$ structure is recovered at large coupling. The role of the long-range Coulomb forces, which is not considered in the main part of the paper, is briefly discussed next. The occurrence of phase separation in real systems is then prevented, and a new CDW with a wave-vector which is not $2k_F$, appears.

3. The adiabatic Holstein model

In this section we recall the definition, and describe early results, relative to the original and extended adiabatic Holstein models [4]. The extended model consists of a single band of electrons linearly coupled to a single optical branch of phonons with dispersion. Within the standard adiabatic approximation used for studying CDW, the quantum kinetic energy terms of the atoms are neglected, because the atoms are supposed to be much heavier than the electrons. In addition, the amplitude of the PLD has to be assumed to be much larger than the amplitude of the zero-point motion of the atoms. The electronic Hamiltonian can be written in the extended form as

$$H(u) = -T \sum_{\langle i,j\rangle\sigma} c_{i\sigma}^{+} c_{j\sigma} + \sum_i \tfrac{1}{2} m\omega_0^2 (u_i^2 - 2\gamma u_{i+1} u_i) + \lambda \sum_i u_i n_i - \mu \sum_i n_i \tag{3}$$

where $u = \{u_i\}$ is the set of lattice distortions which are scalar variables, $c_{i\sigma}^{+}$ and $c_{i\sigma}$ are the creation and annihilation operators of an electron at site i with spin $\sigma = \{\uparrow, \downarrow\}$, $n_i = \sum_\sigma c_{i\sigma}^{+} c_{i\sigma}$ is the electron density operator at site i, $\langle i, j\rangle$ means that the sum is done over all pairs of nearest neighbour sites i, j, λ is the electron–phonon coupling constant, μ is a chemical potential which fixes the band filling, m the mass of each atom, ω_0 the bare phonon frequency, and γ is the parameter that measures the phonon dispersion. The lattice stability requirement implies $|\gamma| < 1/2$. In one dimension, $4T$ is the bandwidth. We first discuss some results obtained in the simplest case $\gamma = 0$, and then describe the case when $\gamma \neq 0$.

3.1. Optical phonons without dispersion $\gamma = 0$

This situation corresponds to the original Holstein model. The ground state of this model is obtained by minimizing $\langle\psi|H(u)|\psi\rangle$ both over the electronic state ψ and u. The extremalization of $\langle\psi|H(u)|\psi\rangle$ with respect to u_i readily yields that the static lattice distortion u_i and the electronic density $\rho_i = \langle\psi|n_i|\psi\rangle = \langle n_i\rangle$ are proportional:

$$u_i = -\frac{\lambda}{m\omega_0^2}\rho_i. \tag{4}$$

The continuum version of this model (where the site index i is taken as a continuous variable x) has been exactly solved by Shastry [12]. A $2k_F$ CDW $\rho(x)$ has been found for all electron–phonon couplings; $\rho(x)$ depends smoothly on the model parameters and there is no phase transition. In the weak-coupling limit, the modulation of the electronic

density $\rho(x)$ is the sine function expected by Peierls–Fröhlich theory. In the strong-coupling limit, $\rho(x)$ exhibits in each period a single sharp peak corresponding to the charge of two electrons. The width of this peak goes to zero as $1/\lambda$. The continuum approximation always yields a Peierls–Fröhlich CDW with a zero-gap phason mode, which is unpinned to the lattice (since the lattice discreteness has been neglected). These CDW can carry a Fröhlich supercurrent.

The continuum approximation breaks down at moderately large coupling when the width of the peaks becomes comparable with the lattice spacing, and then there is phase transition. The numerical studies on a discrete lattice only partially agree with this continuous model. On the one hand, it is confirmed that the CDW ground state indeed remains a $2k_F$ CDW at all couplings. The electronic density can be written as $\rho_i = \rho(2k_F i a + \alpha)$ where $\rho(x)$ is called the hull function [3], a is the lattice spacing and α is an arbitrary phase. On the other hand, we know that the CDW has to become bipolaronic [5] at large enough coupling, and it does. For any band filling ζ, there is a critical coupling $k_c(\zeta)$ for the dimensionless constant

$$k = \lambda \sqrt{\frac{2}{Tm\omega_0^2}} \tag{5}$$

such that the hull function $\rho(x)$ becomes a discontinuous function. This transition appears to be similar in all respects, including the same universality classes for the critical behaviour at the TBA, as those of the Frenkel–Kontorowa model [14].

In this later model, a detailed and exact theory was built. It connects this phenomena with the breaking of Kolmogorov–Arnol'd–Moser tori in the standard map [3]. When ζ is a 'good' irrational number (most of them are 'good'), $k_c(\zeta)$ is non-zero but becomes generally zero when ζ is rational or 'almost rational' (Liouville numbers). This transition is characterized by a gap opening in the phason spectrum and the extinction of Fröhlich conductivity. However, we also find that, at large coupling, the electron density becomes sharply peaked at single sites, as also expected from the result of Shastry.

The strong electron–phonon coupling limit (called atomic by Holstein) is obtained when the bandwidth vanishes ($T = 0$). Because of a formal analogy with the theory of dynamical systems, we relabelled this limit the 'anti-integrable limit' [13]. The Hamiltonian reduces to

$$H_{T=0} = \lambda \sum_i u_i n_i - \mu \sum_i n_i + \sum_i \tfrac{1}{2} m\omega_0^2 u_i^2. \tag{6}$$

Since u_i are scalar variables, the electronic eigenstates of H are those of the operator $n_i = n_{i\uparrow} + n_{i\downarrow}$. We have $\rho_i = 2\sigma_i = (\sigma_{i\uparrow} + \sigma_{i\downarrow})$ with ($\sigma_{i\uparrow} = 0$ or 1, $\sigma_{i\downarrow} = 0$ or 1 and $\sigma_i = 0, 1/2$ or 1).

Because of (4), the total energy can be written as

$$\langle H \rangle_{T=0} = -2U \sum_i \sigma_i^2 - 2\mu \sum_i \sigma_i \tag{7}$$

where

$$U = \frac{\lambda^2}{m\omega_0^2} = \frac{Tk^2}{2} \tag{8}$$

is the binding energy for two polarons forming a bipolaron in the anti-integrable limit. In this limit $T = 0$, we fix $\mu = -U$ in order that the electronic density can be fixed at an arbitrary value, since the energy at a given site is the same either with a bipolaron or with a hole. Without a magnetic field, the existence of polarons $\sigma_i = 1/2$ costs more energy so that the ground state in the atomic limit naturally appears as a degenerate distribution of bipolarons and holes ($\sigma_i = 0$ or 1), which is generally chaotic without long-range order.

The hopping term, which has been neglected in the anti-integrable limit, introduces an interaction between the bipolarons. In the large electron–phonon coupling limit, many standard perturbation theories with respect to the hopping term T (see, for example, [8, 15]) yield, at lowest order, a repulsive interaction between nearest-neighbour bipolarons:

$$\langle H_{\text{eff}} \rangle = \langle H \rangle_{T=0} + \frac{2T^2}{U} \sum_i \sigma_{i+1}\sigma_i. \tag{9}$$

For two bipolarons we pointed out [3] that this interaction remains repulsive at all distances, and decays exponentially as a function of their distance†:

$$\langle H_{\text{eff}} \rangle = \langle H \rangle_{T=0} + \frac{1}{2} \sum_{ij} J_{\text{el}}(i - j)\sigma_i\sigma_j \tag{10}$$

with

$$J_{\text{el}}(n) = \frac{8|n|U}{k^{4|n|}}. \tag{11}$$

(In this notation $((i, j) \neq (j, i)$.) If one neglects the other multispin interactions, which become important for lower electron–phonon couplings, the sequence (11) fulfills at large k, the convexity condition‡

$$J_{\text{el}}(n + 1) + J_{\text{el}}(n - 1) - 2J_{\text{el}}(n) > 0 \qquad \text{for} \quad n \geqslant 2 \tag{12}$$

which implies that the ground state [17–20] is obtained for the sequence of equidistant bipolarons given by (1). The bipolaronic structure is a $2k_F$ CDW, in agreement with [12]. By analogy with exact results obtained in the Frenkel–Kontorowa model [21], we searched and found explicitly from the numerical data in the incommensurate case (see [22] and references therein), a localized form factor function b_n which yields the shape of the electronic density by convolution with the pseudo-spin distribution $\{\sigma_n\}$:

$$\rho_i = \sum_n b_{i-n}\sigma_n. \tag{13}$$

$\{b_n\}$ can be interpreted as the effective shape of the electronic density associated with a bipolaron imbedded in the field of the other overlapping bipolarons. It is positive for all n and decays exponentially for large $|n|$. When $T = 0$, this function b_n reduces to a δ-function at $n = 0$, and has a non-zero width when $T \neq 0$. This bipolaron spreads out and its size diverges at the critical value $k_c(\zeta)$ of the coupling constant k at which the Peierls–Fröhlich CDW is recovered.

† These pseudo-spin interactions will be investigated in detail in the Holstein model in one and two dimensions [16].

‡ More precisely, for $k > 3^{1/4}$, which corresponds to a domain larger than the whole domain where the concept of bipolarons is physically relevant.

3.2. Optical phonons with dispersion: $\gamma \neq 0$

The essential results obtained for the original adiabatic Holstein model at large enough electron–phonon coupling [5] (section 5.3, p 744), extend similarly for the same model with a non-zero dispersion on the optical phonon branch. However, there are some minor differences. There still exist infinitely many chaotic bipolaronic states, but when γ is too large the set of pseudo-spin configurations which labels them has to be 'pruned'.

In other words, there are pseudo-spin configurations $\{\sigma_i\}$ which do not correspond to bipolaronic states. Because of this, the entropy of the whole set of bipolaronic configurations is reduced but, as proven in the above reference, does not vanish.

This pruning effect occurs from the elastic deformations which are created around the bipolarons by the phonon dispersion. A consequence of these deformations is that in the anti-integrable limit $T = 0$, for large enough γ (more precisely, $\gamma > 3/10$, see [5]) there exists certain configurations of bipolarons for which the set of eigenenergies corresponding to the occupied electronic states overlaps the set of energies corresponding to the empty states. A consequence is that these bipolaronic configurations are unstable, because the electrons are not in their ground state. These bipolaronic structures do not exist as a local extrema of the total energy at $T = 0$, so that perturbation theory in T is not possible.

As in the original Holstein model, the critical coupling below which each bipolaronic state disappears still depends on its labelling pseudo-spin configuration $\{\sigma_i\}$, but the upper bound of this critical coupling over all accessible bipolaronic configurations becomes infinite when there is pruning.

However, even in the case with phonon dispersion, the ground state also has to be a bipolaronic structure at large enough electron–phonon coupling. However, then the extra interaction coming from this dispersion competes with the repulsive interaction of electronic origin, described above in the case without phonon dispersion. Unlike J_{el}, it does not vanish in the anti-integrable limit, and thus becomes the essential term at large electron–phonon coupling.

Minimizing the total energy with respect to u_i yields instead of (4), the equation:

$$-\lambda\rho_i - m\omega_0^2\left[u_i - \gamma\,(u_{i-1} + u_{i+1})\right] = 0 \tag{14}$$

which gives

$$u_i = -\sum_j d_{i-j}\rho_j \tag{15a}$$

with

$$d_n = \frac{\lambda\eta_{\mathrm{ph}}^{|n|}}{m\omega_0^2\sqrt{1-4\gamma^2}} \tag{15b}$$

and

$$\eta_{\mathrm{ph}} = \frac{1-\sqrt{1-4\gamma^2}}{2\gamma}. \tag{15c}$$

The lattice distortion $\{u_i\}$ and the electronic density $\{\rho_i\}$ are now related to each other by a convolution with a shape factor $\{d_n\}$ which depends on the details of the phonon

dispersion. In the anti-integrable limit ($T = 0$), $\rho_i = 2\sigma_i$ with $\sigma_i = 0$ or 1, the energy of a bipolaronic configuration $\{\sigma_i\}$ is not degenerate when $\gamma \neq 0$, and becomes

$$\langle H \rangle_{T=0} = -2\mu \sum_i \sigma_i + \frac{1}{2} \sum_{i,j} J_{\mathrm{ph}}(i-j)\sigma_i\sigma_j \tag{16a}$$

with

$$J_{\mathrm{ph}}(n) = -\frac{4U}{\sqrt{1-4\gamma^2}} \eta_{\mathrm{ph}}^{|n|}. \tag{16b}$$

Note that (16*a*) represents the energy of a bipolaronic configuration $\{\sigma_i\}$ in the case that it exists as a metastable state. When γ is positive, $J_{\mathrm{ph}}(n)$ is always negative, while it has an alternate sign when γ is negative. For the sake of simplicity, we choose to study the situation with γ positive, which corresponds to a ferromagnetic interaction in (16*a*) at all distances. Then, choosing the chemical potential $\mu = -U$ in order to fix the band filling at an arbitrary number ζ, the ground state of a large system of size L, is obtained by a phase separation in two domains, for example:

$$\sigma_i = 1 \qquad 0 < i < \zeta L \tag{17a}$$

$$\sigma_i = 0 \qquad \zeta L < i < L. \tag{17b}$$

When the transfer integral T is not zero, the effective repulsion between bipolarons calculated in (11) appears and competes with the bipolaron attraction (16*b*). This term increases as T increases or, equivalently, as the electron–phonon coupling λ becomes smaller. Since at low electron–phonon coupling the Peierls–Fröhlich instability appears very precisely as a $2k_F$ CDW, it is an interesting question to understand how the CDW evolves between these two regimes.

4. Systems with one and two bipolarons: numerical analysis

In the regime of intermediate electron–phonon coupling, it becomes much more difficult to analyse the interactions between the bipolarons than when close to the limit $T = 0$. These interactions cannot be strictly split as the sum of several pair contributions because multispin interactions are also involved. Numerical calculations, which integrate globally all contributions to the interaction energy, are much more reliable. Our numerical method consists in following continuously bipolaronic configurations characterized by $\{\sigma_i\}$ and its energy known in the limit $T = 0$ as a function of T.

The details of our technique were described in appendix A of [22], although it was applied there to a different problem involving both bipolarons and polarons. Let us first analyse the structure of a single bipolaron and the interaction between two bipolarons when there is a phonon dispersion.

4.1. Single bipolaron

For a single bipolaron (for example, at site 0), the electronic eigenstate $\{\varphi_n\}$ is doubly occupied and its eigenenergy E_{el} is determined by the 'self-consistent eigenequation'

$$-T\varphi_{n+1} - T\varphi_{n-1} + \lambda u_n \varphi_n = E_{el}\varphi_n \tag{18}$$

where the lattice distortion u_n is related to the electronic density $\rho_n = 2|\varphi_n|^2$ by the convolution (15*a*) with a shape factor $\{d_n\}$. Since for a single bipolaron u_n goes to zero as $|n|$ goes to ∞, the electronic density ρ_n behaves as $\exp(-\kappa_{el}|n|)$ for large n with

$$\kappa_{el} = \frac{1}{\xi_{el}} = \frac{-E_{el} + \sqrt{E_{el}^2 - 4T^2}}{T}. \tag{19}$$

Because of (15*a*), u_n also behave as $\exp(-\kappa_u|n|)$ with $\kappa_u = 1/\xi_u$. Since $d_n \propto \exp(-\kappa_{ph}|n|)$ with $\xi_{ph} = 1/\kappa_{ph}$, the result of the convolution (15*a*) yields

$$\xi_u = \mathrm{Max}(\xi_{el}, \xi_{ph}). \tag{20}$$

A single bipolaron exhibits two characteristic sizes, which are ξ_{el} for its electronic density and ξ_u for its lattice distortion. These two sizes become equal at small enough electron–phonon coupling because, in (20), ξ_{el} diverges while ξ_{ph} remains constant. On the other hand, at large coupling they must be unequal because ξ_{el} goes to zero. There is a transition point at some critical value of the electron–phonon coupling $k_{cd}(\gamma)$.

These characteristic lengths were measured on our numerical data as a function of k.

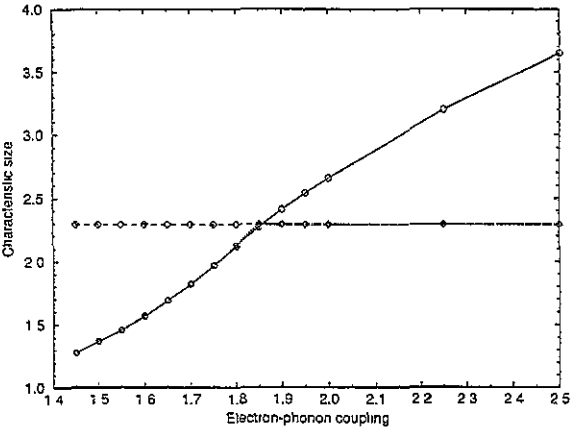

Figure 1. Inverse electronic size κ_{el} (full curve and lattice distortion size κ_u (dotted curve) as a function of the electron–phonon coupling, for $\gamma = 0.1$, compared to the constant κ_{ph} (broken line).

The plot of figure 1, done for a relatively small phonon dispersion $\gamma = 0.1$, clearly shows this transition. Figure 2 shows $k_{cd}(\gamma)$. This transition line roughly determines the cross-over region where the range of the electronic interaction J_{el} becomes shorter than the range of the elastic interaction J_{ph}.

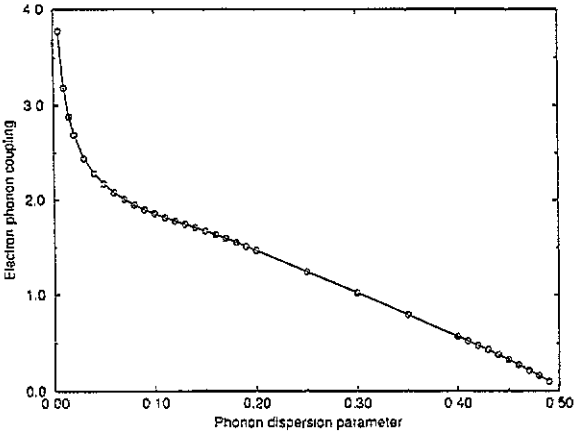

Figure 2. Critical electron–phonon coupling $k_{cd}(\gamma)$ as a function of the phonon dispersion parameter γ.

4.2. Interaction between two bipolarons

Let us now calculate numerically the effective pair interaction $J(n)$ between two bipolarons as a function of their distance (in a system with only two bipolarons). The results are reported in figure 3(*a*).

For a moderately small value of the electron–phonon coupling $k = 2$ in the bipolaronic regime†, and for small values of the dispersion parameter $\gamma < 0.05$, the interactions between the bipolarons remain repulsive at all distances (i.e. equation (12) is fulfilled). The ground state is achieved when the bipolarons are equidistant, which yields a $2k_F$ CDW.

For all other positive values of γ, the interaction energy versus the distance between the bipolarons is not a convex function because the elastic interaction mediated by the dispersion becomes more important. For $\gamma > 0.15$, the minimum of $J(n)$ is at $n = 1$. This situation favours the phase separation that exists in the anti-integrable limit‡. For the intermediate values of γ the minimum of $J(n)$ is located between 2 and ∞. Other phase separations are favoured in that case.

A more complete view is reported on figure 3(*b*) in the phase diagram (k, γ), where the domains of absolute minima of $J(n)$ are shown.

The two extreme domains correspond to a minimum of $J(n)$ at $n = 1$ (upper part of the figure), and to a $2k_F$ CDW (lower part of the figure); in between some intermediate domains are also shown, which correspond to minima of $J(n)$ between $n = 1$ and $n = \infty$.

These results with two bipolarons prove the existence of phase separations in the non-overlapping bipolaronic structure at low enough density, when mostly pair interactions play a role. When the density of bipolarons become large and when they overlap it is more accurate to make a direct calculation of the global structure and of its energy in order to get the ground state.

5. Systems with many bipolarons: numerical analysis

At large coupling, we know that systems with many electrons exhibit infinitely many

† For $k \geqslant k_c \sim 1.58$ there is no Peierls–Fröhlich CDW at any band filling for $\gamma = 0$.

‡ Remember that, because of the Pauli principle, two bipolarons cannot occupy the same site.

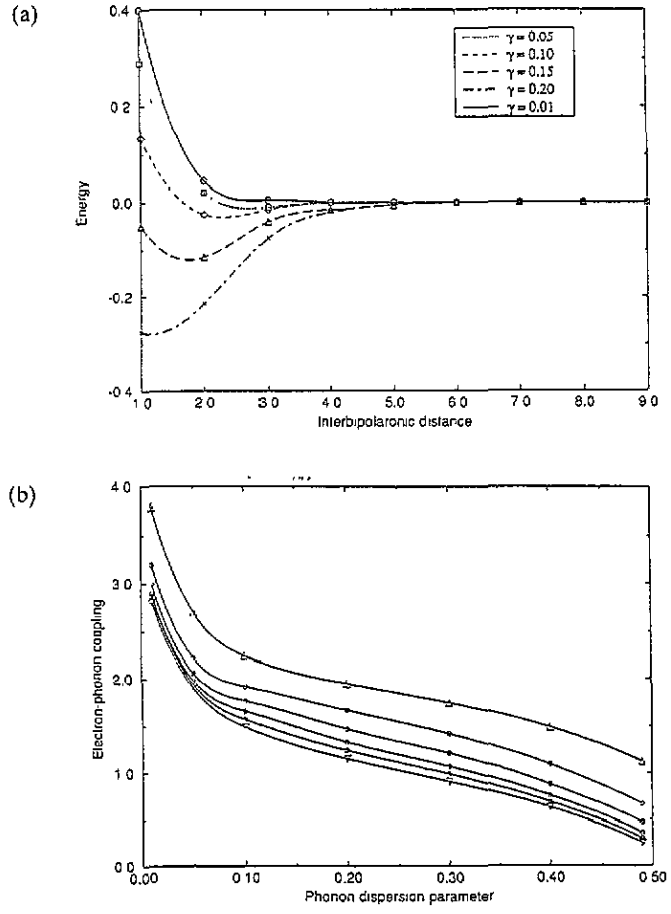

Figure 3. (*a*) Interaction energy of two bipolarons as a function of their relative distance for various phonon dispersion parameter γ, and for $k = 2.0$. (*b*) Domains of absolute minima of the bipolaron interaction in the (k, γ) plane (see comment in text).

bipolaronic structures represented by pseudo-spin configurations $\{\sigma_i\}$, among which the ground state lies. For a large but finite system with N sites, this number grows as $\exp(\beta N)$, where β is some positive non-zero 'entropy'. When there is no pruning ($\gamma < 3/10$, see [5]), this entropy is just $\beta = \mathrm{Ln}\,2$. The consequence is that, even when N is reasonably large, the number of bipolaronic configurations which have to be checked in order to find the ground state becomes huge and exceeds our numerical capabilities. To find the ground state, we restrict the family of bipolaronic configurations that are tested with empirical arguments, which we now describe.

5.1. Structure of the phase diagram in the vicinity of a multiphase point

At the point ($T = 0$, $\gamma = 0$, $\mu = -U$) of the phase diagram, the energy of a bipolaron is exactly zero, and the interaction energies between bipolarons also strictly vanish. Any bipolaronic configuration is a ground state, which thus is totally degenerate. Such a point in the phase diagram is a 'multi-phase point', similar to those found in the ANNNI model [23, 24] and other models.

Let us describe the scheme which usually works for describing the vicinity of a multiphase point when its degeneracy is raised by some perturbations. We do not specify the model and the type of perturbation, but review and reformulate the essential and general ideas.

A standard multiphase point is at the border between two domains of stability in the phase diagram of two periodic phases with unit cells labelled $\{A\}$ and $\{B\}$ respectively. At the multiphase point, the degenerate structure is described by random sequences of blocks $\{W_i\}$, where W_i is arbitrarily $\{A\}$ or $\{B\}$. This degeneracy implies that (i) the energy per site of the pure phases A and B are the same; (ii) the average energy $(E_{AB} + E_{BA})/2$ of the interface $\{\cdots AAABBB\cdots\}$ between the two periodic phases with unit cells $\{A\}$ and $\{B\}$ respectively, and of the interface $\{\cdots BBBAAA\cdots\}$ in reverse order, is zero; and (iii) the interfaces do not interact, whatever their relative distance.

When a perturbation is added to the Hamiltonian, its effect on the degenerate multiphase point is treated recursively at all orders of the perturbation. The degeneracy of the multiphase point is usually raised at the lowest significant order by the perturbation, and becomes a transition point characterized by equal energies per site of the pure phases A and B. At this transition point, the average energy of the interface $(E_{AB} + E_{BA})/2$ can become either positive or negative, which corresponds to the following two different situations.

In the first situation, **F**, the average energy of the interfaces $(E_{AB} + E_{BA})/2$ becomes positive after the perturbation. Then, only pure phases A or B can be stable at the transition point. In that case, the multiphase point just becomes, after perturbation, a standard first-order transition between the periodic phase with unit cell $\{A\}$ and the other periodic phase with unit cell $\{B\}$.

In the second situation, **D**, the average energy of the interfaces $(E_{AB} + E_{BA})/2$ becomes negative after the perturbation. The interaction energies between these interfaces are of higher order in perturbation, and can be dropped at the lowest order. Then, the intermediate phase with unit cell $\{AB\}$ obtained by juxtaposition of $\{A\}$ and $\{B\}$ becomes the most stable, not only at a single point but in a non-vanishing domain, because the density of interfaces lowering its free energy is maximum. This new phase domain is inserted between the stability domain of the periodic phase with unit cell $\{A\}$ and the stability domain of the periodic phase with unit cell $\{B\}$, with an end point at the initial multiphase point where the perturbation is zero.

At the border between the stability domain of the periodic phase with unit cell $\{A\}$ and the periodic phase with the unit cell $\{AB\}$, there is a new multiphase point where the degenerate structure consists in a random sequence of blocks $\{W_i\}$ where either $W_i = \{A\}$ or $W_i = \{AB\}$. There is also a second multiphase point with degenerate structure $\{W_i\}$, where either $W_i = \{AB\}$ or $\{W_i\} = \{B\}$ at the border between the periodic phase with unit cell $\{AB\}$ and the periodic phase with unit cell $\{B\}$.

To have this scheme, a part of the perturbation that consists of the highest-order terms has been dropped. These terms are considered as a new perturbation of the obtained phase diagram. We repeat the above analysis for each of the two new multiphase points. Each of them could become (independently) either a first-order transition, or generate an intermediate phase with two multiphase points, and so on. The construction of the phase diagram can be done recursively following this algorithm.

The validity of this recursive treatment of multiphase points requires an explicit calculation of the perturbation at increasing order. This was implicitly done in [25], which focuses on a problem at finite temperature. Taking the zero-degree limit in that paper, the recursive construction of the phase diagram of the ground state of an Ising spin model with antiferromagnetic long-range interactions, was obtained. In that case, situation **F** never

occurs at any order of the recursive analysis of the multiphase point and, consequently, there are no first-order transitions in the phase diagram for that model. The resulting phase diagram of this model contains all the possible phases that can be labelled by 1. It is an alternative method for recovering the Devil's staircase, which was known to exist in the considered model. In other models, such as the ANNNI model [24], situation **F** occurs at some level of the scheme, but there are also branching points where first-order transition points become multiphase points.

This validity of the above 'two-blocks' scheme for analysing a multiphase point may fail if the successive order of the perturbation terms does not decay smoothly or fast enough. This analysis also fails if the multiphase point itself corresponds to higher degeneracy where, for example, three (or more) different phases with unit cells $\{A\}$, $\{B\}$ and $\{C\}$ mix together arbitrarily. We have the example where a two-block construction of the ground state fails and where the recursive construction requires three blocks [26, 27]. Then, one get more complicated structures which may be neither periodic nor quasi-periodic but only weakly periodic (e.g. see [27]).

5.2. Farey construction of phases in the vicinity of a multiphase point

Any of the unit cells of the periodic phases which are obtained within this scheme can be constructed from two initial 'blocks' $\{A\}$ and $\{B\}$ with the help of the two inflation rules $\mathcal{T}_L$ and $\mathcal{T}_R$, which define two new blocks $\{A'\}$ and $\{B'\}$ by

$$(\{A'\},\{B'\}) = \mathcal{T}_L(\{A\},\{B\}) \tag{21a}$$

with

$$\{A'\} = \{A\} \qquad \{B'\} = \{AB\} \tag{21b}$$

and

$$(\{A'\},\{B'\}) = \mathcal{T}_R(\{A\},\{B\}) \tag{22a}$$

with

$$\{A'\} = \{AB\} \qquad \{B'\} = \{B\}. \tag{22b}$$

We characterize all possible structures which can be obtained with these rules.

Let us ascribe to the initial unit cells $\{A\}$ and $\{B\}$, the code 0 and 1 respectively. Infinite pseudo-spin sequences $\{\sigma_i\}$ are generated by all arbitrary products of a transformation $\mathcal{T}_l$, where either $\mathcal{T}_l = \mathcal{T}_L$ or $\mathcal{T}_l = \mathcal{T}_R$, applied to each of these initial states. When the sequence of $\mathcal{T}_l$ is finite, the obtained sequence $\{\sigma_i\}$ is repeated periodically in both directions, which makes it an infinite sequence. According to [25], each of these infinite sequences $\{\sigma_i\}$, is described by 1 with an appropriate choice of the number ζ and of the phase α. The sequence of block transformations $\mathcal{T}_l$ is uniquely determined by the continued fraction expansion of ζ. It is finite if and only if ζ is rational, and then $\{\sigma_i\}$ is periodic. The consequence of this result is that the perturbations at a standard multiphase point can only yield the commensurate and incommensurate phases associated with pseudo-spin sequences among those given by 1.

All possible unit cells $\left[\prod_{n=1}^{N} \mathcal{T}_n\right]\{i\}$ with $\{i\} = \{0\}$ or $\{1\}$ and N finite, and their corresponding rational ζ, are obtained within a construction that follows in parallel the standard Farey construction of rational numbers in the interval [0, 1] at order N.

We start initially ($N = 0$) from the line consisting of the sequence of two rationals $\zeta = 0/1$ and $\zeta = 1/1$ which are associated with the unit cell $\{0\}$ and $\{1\}$ respectively, and we apply recursively the following algorithm.

Let us consider the Nth line which consists of a sequence $\{r_n^N/s_n^N\}$ of rationals (where n runs from $n = 1$ to $n = 2^N + 1$), so that the corresponding periodic sequences 1 have a unit cell denoted $\{\mathrm{Cell}_n^N\}$†. Then, we construct the next $(N+1)$th line which contains $2^{N+1} + 1$ rationals, as a new sequence of rationals obtained by inserting between every pair of consecutive rationals r_n^N/s_n^N and r_{n+1}^N/s_{n+1}^N of the old sequence, the new rationals $(r_n^N + r_{n+1}^N)/(s_n^N + s_{n+1}^N)$. The unit cell of the sequence 1 associated with this rational number is just obtained as the juxtaposition $\{\mathrm{Cell}_n^N \mathrm{Cell}_{n+1}^N\}$ of the two parent unit cells.

It has been proven [28] that all the rational numbers in the interval $[0, 1]$ are obtained in their irreducible form by this construction, and appear once and only once in each line when N is large enough.

To be clearer, let us describe explicitly how these rules work for the first lines of the Farey construction. The first line ($N = 1$) is $\{\frac{0}{1}, \frac{1}{2} = \frac{0+1}{1+1}, \frac{1}{1}\}$ where the new rational $\zeta = 1/2$ is associated with the unit cell $\{01\}$.

The second line ($N = 2$) is $\{\frac{0}{1}, \frac{1}{3} = \frac{0+1}{1+2}, \frac{1}{2}, \frac{2}{3} = \frac{1+1}{2+1}, \frac{1}{1}\}$. The two new rationals $\zeta = 1/3$ and $2/3$ are associated with the unit cells $\{001\}$ and $\{011\}$ respectively, and so on.

For any rational number $\zeta_r = r/s$ (in irreducible form), there exists a smallest N such that ζ_r belongs to all lines with order $l > N$ in the Farey construction. It can be written uniquely as $(r_n^N + r_{n+1}^N)/(s_n^N + s_{n+1}^N)$. The two rational numbers r_n^N/s_n^N and r_{n+1}^N/s_{n+1}^N are called the two parents of ζ_r. They can also be obtained from the standard continued fraction expansion of $0 < \zeta_r < 1$

$$\zeta_r = \cfrac{1}{a_1 + \cfrac{\cdots}{a_{N-2} + \cfrac{1}{a_{N-1} + \cfrac{1}{a_N + \frac{1}{1}}}}} \tag{23}$$

with integer coefficients $1 \leqslant a_i$. By convention, the last integer coefficient a_{N+1} in this expansion is 1.

The two parents of ζ_r are

$$\zeta_{r_1} = \cfrac{1}{a_1 + \cfrac{\cdots}{a_{N-2} + \cfrac{1}{a_{N-1} + \frac{1}{a_N}}}} \tag{24}$$

$$\zeta_{r_2} = \cfrac{1}{a_1 + \cfrac{\cdots}{a_{N-2} + \frac{1}{a_{N-1}}}} \tag{25}$$

and are ordered by convention such that the first one ζ_{r_1} has the largest denominator.

The second generation of parents of ζ_r is the pair of consecutive integers of the next upper line $N - 1$ of the Farey construction, the interval of which contains ζ_r. These two numbers are the parents of ζ_{r_1} and are, when $a_N > 1$,

$$\zeta_{r_3} = \cfrac{1}{a_1 + \cfrac{\cdots}{a_{N-2} + \cfrac{1}{a_{N-1} + \frac{1}{a_N - 1}}}} \qquad \zeta_{r_2} \tag{26}$$

† This is a particular determination of the unit cell, which is not unique and depends on the phase α in **1**.

and are, when $a_N = 1$,

$$\zeta_{r_2} \qquad \zeta_{r_3} = \frac{1}{a_1 + \frac{1}{\cdots + \frac{1}{a_{N-2}}}}. \tag{27}$$

At the second generation ζ_r keeps only two parents, and so on.

If $a_N = 1$ both ζ_{r_2} and ζ_{r_3} are principal convergent of ζ_r, while if $a_N > 1$, ζ_{r_2} is a principal convergent but ζ_{r_3} is only an intermediate convergent of ζ_r. One recognizes here that this sequence of nth generation parents of a rational number just coincides with the sequence of pairs of intermediate and principal convergents considered in [25]. This sequence becomes infinite for an irrational number, which has an infinite continued fraction expansion.

These parent commensurate structures play a role in the interpretation of the phase separations that were numerically observed (see sections 5.3 and 5.4).

5.3. Phase separation in the bipolaronic phase diagram

Turning back to our adiabatic Holstein model with dispersion, we noted that the special point ($T = 0, \gamma = 0, \mu = -U$) is a multiphase point in the phase diagram of the ground state versus T, γ, μ. This point is at the border line between the phase characterized by the pseudo-spin sequence $\sigma_i = 0$ for all i and the phase characterized by $\sigma_i = 1$ for all i. With $\{A\} = 0$ and $\{B\} = 1$, the bipolaronic configurations labelled with the pseudo-spin sequences (1) represent the whole set of configurations that could be obtained by this multiphase scheme.

Although we have no rigorous proof, we think that we should find the true ground states in this set for two reasons. On the one hand, at large electron–phonon coupling that is close to the multiphase point, the characteristic length of the interaction between the bipolarons goes to zero. As a result, successive orders of the perturbation series should go to zero very quickly. This is the ideal situation where the standard analysis described above works. On the other hand, in the opposite limit at low electron–phonon coupling, the bipolaronic configurations corresponding to (1) just become the whole set of Peierls–Fröhlich CDW obtained for all band filling, which we observed numerically below the TBA.

Our numerical technique consists in following by continuity each of these bipolaronic configurations, which are explicitly known in the anti-integrable limit, and to calculate its energy. In practice, we start from $k = \infty$ and $\gamma = 0$ for a given (rational) band filling

$$\zeta = \frac{1}{2N} \sum_i \langle n_i \rangle$$

(k, γ and ζ are the dimensionless parameters of the model, and N the total number of sites) and we vary by small steps either k or γ or both in order to follow a continuous path. It might happen that the solution is lost because a discontinuity (even a small discontinuity) is observed in the configuration $\{u_i\}$. However, this situation never happens when $\gamma = 0$. Then, if a given point (k, γ) in the phase diagram can be reached continuously, it is more efficient to vary k and then γ. In any case, if the configuration exists it is the same for any continuous path used for calculating it. If this point cannot be reached by any continuous path, we conclude that the corresponding configuration (likely) does not exist (pruning) and thus can be discarded in the energy tests. In practice, only commensurate systems can be studied, but their commensurability order can be chosen to be as large as needed.

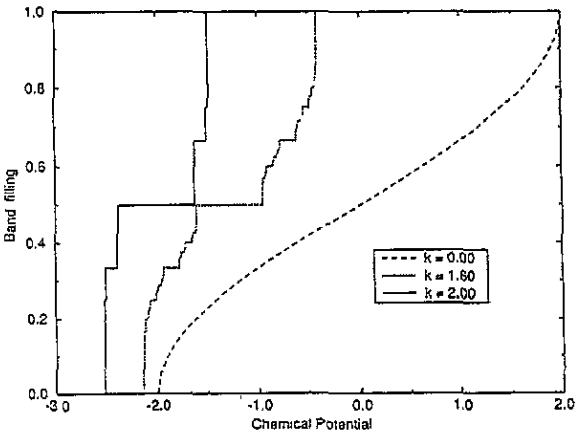

Figure 4. Band filling as a function of the chemical potential μ for $\gamma = 0$, and for different values of the electron–phonon coupling k.

The energy per site which is obtained for each configuration for a given band filling does not depend on the system size, when the system is large enough. In practice, about 100 sites appears to be sufficient to obtain reasonable accuracy in energy (better than 10^{-6}). This average energy is calculated for commensurate systems with band filling $\zeta_r = r/s$ for all rationals with denominators $s \leqslant 15$. For that purpose, the configuration $\{u_i\}$ and its energy is calculated for a system of ns sites with nr electron pairs. The integer n is chosen in order that ns be about 100.

The ground state is the configuration which has the lowest energy per site. Fixing the sequence of pseudo-spins (1) determines a bipolaronic structure as a continuous function of k and γ which is independent of μ. For a given set (k, γ), the energy (3) per site of this structure is a function of ζ and μ, which can be written as

$$\Psi_\mu(\zeta) = \Psi_0(\zeta) - 2\mu\zeta. \tag{28}$$

The density of electrons $\zeta(\mu)$ is determined as a function of μ by minimizing $\Psi_\mu(\zeta)$ with respect to ζ. If $\Psi_0(\zeta)$ is a convex function of ζ, this function is given implicitly by the equation

$$\frac{\partial \Psi_0(\zeta)}{\partial \zeta} = 2\mu. \tag{29}$$

The electron–hole symmetry of the Hamiltonian (3) implies, after some calculations, that the function

$$\Psi_0(\zeta) - 2\mu_0\zeta = \Psi_0(1-\zeta) - 2\mu_0(1-\zeta) \qquad \text{with} \qquad \mu_0 = -\frac{\lambda^2}{(1-2\gamma)m\omega_0^2} \tag{30}$$

is symmetric with respect to the point $\zeta = 1/2$. It is sufficient to study the band fillings between 0 and $1/2$, and to complete the calculations by symmetry.

When there is no dispersion ($\gamma = 0$), $\Psi_0(\zeta)$ is convex for any value of the electron–phonon coupling k. Its derivative has a discontinuity at every rational so that the function $\zeta(\mu)$ is a continuous and monotonous increasing curve with a constant plateau at each rational. This curve is a Devil's staircase, which is expected to be complete above the critical values $k > \max_\zeta k_c(\zeta)$ and incomplete below (see figure 4).

It is found that the function $\Psi_0(\zeta)$ always becomes non-convex for any electron–phonon coupling k, providing the dispersion coefficient γ becomes large enough (and of course smaller than 1/2). To study the phase separations occurring when the function $\Psi_0(\zeta)$ is non-convex, it is convenient to define its convex envelope $\Psi_{env}(\zeta)$ as

$$\Psi_{env}(\zeta) = \min_{\zeta_1<\zeta,\,\zeta_2>\zeta} \Psi_0(\zeta_1)\frac{\zeta_2-\zeta}{\zeta_2-\zeta_1} + \Psi_0(\zeta_2)\frac{\zeta-\zeta_1}{\zeta_2-\zeta_1} \tag{31}$$

and the difference between this function and its convex envelope

$$\Delta(\zeta) = \Psi_0(\zeta) - \Psi_{env}(\zeta) \geqslant 0 \tag{32}$$

which is positive or zero. The numerical calculation of $\Delta(\zeta)$ yields very sensitive information about the phase separations in the model.

Three regimes occur for a given k (see figure 5).

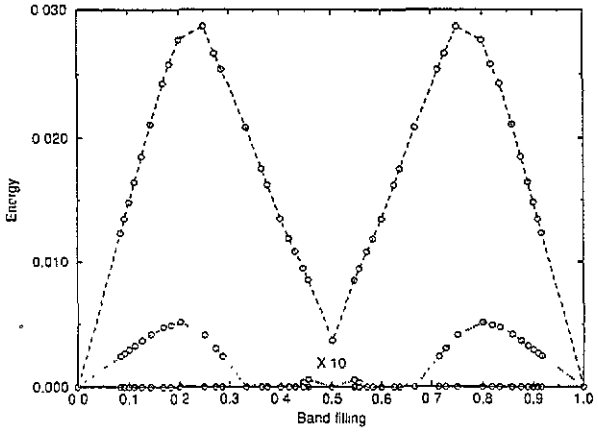

Figure 5. $\Delta(\zeta)$ as a function of band filling for $k = 1.70$. The three curves correspond to $\gamma = 0.05$ (full curve), $\gamma = 0.16$ (dotted curve) and $\gamma = 0.22$ (broken curve).

In the first situation, for small enough γ (the case $\gamma = 0.05$ is shown in figure 5), the function $\Delta(\zeta)$ is found to be identically zero and then $\Psi_0(\zeta)$ is surely a convex function. The function $\zeta(\mu)$ defined by (29) is a Devil's staircase.

In the second situation when γ becomes larger, the function $\Delta(\zeta)$ becomes non-zero (the dotted curve, $\gamma = 0.16$, in figure 5). We observe that it is non-zero in one or several non-overlapping open intervals I_ν, while it is zero outside. In addition, the ends of each of these intervals often (but not always) correspond to rational numbers which can be associated one with another as 'parents', according to definitions (24) and (25). If the band filling is fixed to a given number ζ, which belongs to an interval $I_\nu =]\zeta_-, \zeta_+[$, the ground state is not the bipolaronic configuration labelled by (1). There is a phase separation in two domains with different band filling ζ_- and ζ_+ both labelled by (1) with their respective values of ζ. On the other hand, if ζ does not belong to any of the interval I_ν, there is no phase separation and the ground state remains the bipolaronic configuration labelled by (1).

The third situation occurs when γ is large enough and becomes close to 1/2 (see for example $\gamma = 0.22$; the broken curve in figure 5). Then, $\Delta(\zeta)$ becomes non-zero in the

whole interval]0, 1[. There are phase separations for any value of $\zeta \neq 0$ and $\neq 1$ into two domains. In one of the domains, the electronic band is empty, $\sigma_i = 0$ for all i, and in the second domain the electronic band is full, $\sigma_i = 1$ for all i.

Figure 6 shows the global regions in the phase diagram (k, γ), where (i) $\Delta(\zeta)$ is zero in the whole interval [0, 1] (below the full curve in figure 6). Any band filling yields a stable CDW. There is no phase separation at any band filling. (ii) $\Delta(\zeta)$ is non-zero, at least for one ζ (between the full and dotted curves in figure 6). (iii) $\Delta(\zeta)$ is non-zero for all $\zeta \neq 0$, $\zeta \neq 1/2$ and $\zeta \neq 0$. Only the band fillings $0, 1/2$ and 1 yield stable CDW (between the dotted and broken curves in figure 6). For any other band filling ζ, there is a phase separation into two domains corresponding to a domain with a half-filled band and a domain either with an empty band or with a full band. (iv) $\Delta(\zeta)$ is non-zero for all $\zeta \neq 0$ and $\zeta \neq 1$ (above the broken curve in figure 6). For any band filling ζ, there is a phase separation into a domain with an empty band and a domain with a full band.

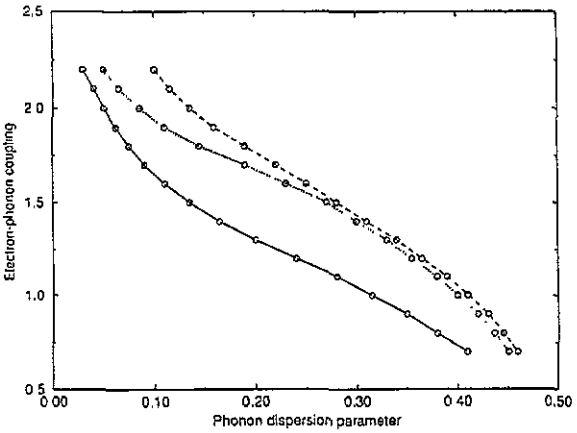

Figure 6. Domains of variation of $\Delta(\zeta)$ in the plane (k, γ) (see comments in the text).

For a given irrational $\zeta = \frac{3-\sqrt{5}}{2}$ (in practice, a rational with a large denominator which is a best approximation of this number, for example $\zeta = 34/89$), figure 7 shows the phase diagram (k, γ). (i) The domain where the ground state is a Peierls–Fröhlich CDW (analytic hull function). (ii) The domain where the ground state is a bipolaronic CDW (with discontinuous hull function) with no phase separation. (iii) The domain where there is a phase separation.

There is an apparently infinite cascade of phase separations inside this domain with transition lines that accumulate on the boundary of the stable domain of the incommensurate CDW.

Considering a given rational band filling $\zeta_r = r/s$, varying γ from zero, one necessarily obtains a phase separation at some critical point. It is interesting to note that in many cases (but not in all cases), the phase separation occurs between the two parent commensurate phases which are the bipolaronic structures labelled by (1) obtained for the two parent rational numbers of ζ. For larger γ, there is another phase separation into the next parent phase and so on until the complete separation in phase {0} and {1}. For example, figure 8 shows magnifications where the commensurate phase with $\zeta = 5/11$ separates into the two

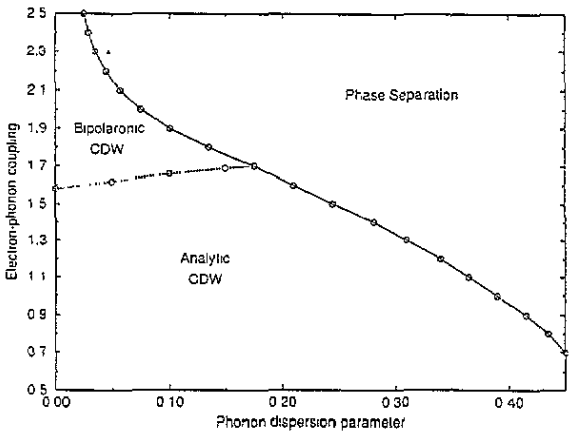

Figure 7. Phase diagram in the (k, γ) plane.

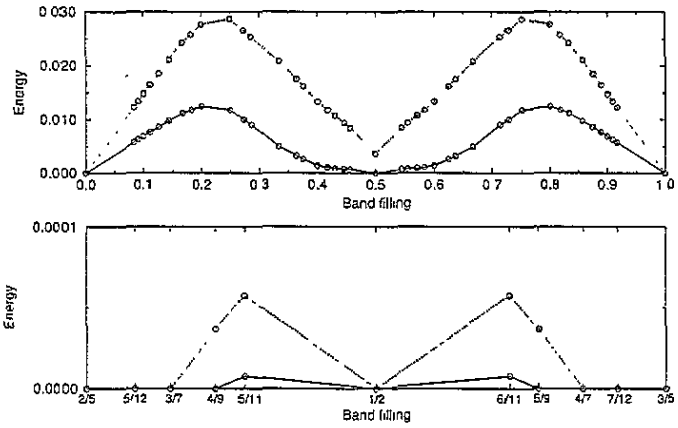

Figure 8. Separation of the commensurate phase 5/11 for $k = 1.70$ into its parent phases (lower figure: $\gamma = 0.12$ (full curve) and $\gamma = 0.16$ (dotted curve)) or into its non-parent phases (upper figure: $\gamma = 0.19$ (full curve) and $\gamma = 0.22$ (dotted curve)).

parent phases with $\zeta_- = 4/9$ and $\zeta_+ = 1/2$, then into the next parent phases $\zeta_- = 3/7$ and $\zeta_+ = 1/2$ (lower figure).

Continuing to increase γ we did not observe phase separations, neither into the parent phases $\zeta_- = 2/5$ and $\zeta_+ = 1/2$ nor into the next pair of parent phases $\zeta_- = 1/3$ and $\zeta_+ = 1/2$, but instead we observed directly the phase separation into two phases with $\zeta_- = 0/1$ and $\zeta_+ = 1/2$ and finally with $\zeta_- = 0/1$ and $\zeta_+ = 1/1$ (upper figure in figure 8).

Another example is $\zeta = 1/3$, which does not follow this criteria of parent phases. The successive phase separation occurs between $\zeta_- = 0/1 = Cste$ and $\zeta_+ = 4/11$, then with $\zeta_+ = 3/8$, $\zeta_+ = 2/5$, $\zeta_+ = 4/9$, $\zeta_+ = 1/2$ and finally $\zeta_+ = 1/1$.

5.4. A toy model for the bipolaronic phase separations

An understanding of these cascades of phase separations requires a detailed knowledge of the

interactions between bipolarons for every value of the parameters of the model, knowledge which we do not have. For a better understanding of the obtained results, it is useful to introduce a 'toy' model that can mimic some of the observed behaviour. It is simply a schematic pseudo-spin model with Hamiltonian

$$H = \frac{1}{2}\sum_{i,j} J(i-j)\sigma_i\sigma_j - 2\mu\sum_i \sigma_i \tag{33}$$

where $\sigma_i = 0$ or 1 and the pair interactions $J(n) = J_{el}(n) + J_{ph}(n)$ for two bipolarons at distance n. Only pair interactions between the bipolarons are taken into account as the sum of two competing terms according to the qualitative ideas suggested in section 2. The first term $J_{el}(n)$ represents the interaction due to the overlap between the electronic wavefunctions of the bipolarons. It is supposed to be repulsive at all distances. The second term $J_{ph}(n)$ represents the interaction due to the phonon dispersion. When $\gamma > 0$, this contribution is attractive at all distances. Both interactions should decay exponentially as a function of $|n|$, but with a different rate. We propose the following simple choice:

$$J_{el}(n) = J_1\eta_{el}^{|n|} \tag{34}$$

$$J_{ph}(n) = -J_2\eta_{ph}^{|n|} \tag{35}$$

with J_1 and J_2 positive. This Hamiltonian contains four parameters, J_1, J_2, η_{el}, η_{ph}, which should depend in some complex way on those of the initial Hamiltonian. The limit point $\eta_{el} = \eta_{ph} = 0$ and $\mu = \mu_0 = \frac{1}{4}J(0)$ is a multiphase point which can be formally analysed as explained above. We just have to select the ground state of (33) among the sequence (1) where the parameter ζ is determined by minimizing the average energy per site of (33)

$$\Psi_\mu(\zeta) = \Psi_0(\zeta) - 2\mu\zeta = \frac{1}{2}\sum_n K(n)\varphi(n\zeta) - 2(\mu-\mu_0)\zeta \tag{36}$$

where $K(n) = J(n+1) + J(n-1) - 2J(n)$ and $\varphi(\alpha)$ is defined [20] as the continuous function

$$\varphi(x) = x\,\mathrm{Int}(x) - \tfrac{1}{2}\mathrm{Int}(x)(\mathrm{Int}(x)+1). \tag{37}$$

The derivative $\frac{\partial\Psi_0(\zeta)}{\partial\zeta}$ has a right determination $\Psi_0'^{+}(\zeta)$ and a left determination $\Psi_0'^{-}(\zeta)$:

$$\Psi_0'(\zeta) = \frac{1}{2}\sum_n nK(n)\mathrm{Int}(n\zeta) = \sum_{n>0} nK(n)(\mathrm{Int}(n\zeta) + \tfrac{1}{2}) \tag{38}$$

corresponding to the left and right determination of the function integer part of x (Int (x)) respectively. $\Psi_0'(\zeta)$ is just a sum of step functions with discontinuities at every rational. The amplitude of the discontinuity at $\zeta = r/s$ where r and s are irreducible integers depends only on s:

$$\Psi_0'^{+}(\zeta) - \Psi_0'^{-}(\zeta) = \delta(s) = \sum_{n>0} nsK(ns). \tag{39}$$

When $J(n)$ is a convex function of n, i.e when (12) is fulfilled, $K(n)$ is positive for all n and this derivative is monotone increasing. The function $\Psi_0(\zeta)$ is convex and the curve

$\zeta(\mu)$ which is implicitly determined by $\Psi_0'(\zeta) = 2(\mu - \mu_0)$ is a complete Devil's staircase. The width of the plateaus at rational $\zeta = r/s$ is given by (39) as $\frac{1}{2}\delta(s) > 0$. Then, it was indeed proven rigorously [17–20] that the ground state is given by the sequence (1) and that $\zeta(\mu)$ is a complete Devil's staircase.

When $J(n)$ is not a convex function,

$$\delta(s) = J_1(\eta_{el} + \eta_{el}^{-1} - 2)s\frac{\eta_{el}^s}{(1-\eta_{el}^s)^2} - J_2(\eta_{ph} + \eta_{ph}^{-1} - 2)s\frac{\eta_{ph}^s}{(1-\eta_{ph}^s)^2} \quad (40)$$

may become negative for some values of s. The function $\Psi_0(\zeta)$ is non-convex if and only if $\delta(s)$ is negative for some values of s.

$\Psi_0(\zeta)$ may become non-convex in different ways. Below we describe two of them.

Example 1

$\delta(s)$ can first become negative for large $s > S$ where the integer bound S is assumed to decrease from ∞ when the model parameter varies beyond the threshold of convexity. There are phase separations which first occur for the incommensurate phases and the high-order commensurate phases in decreasing order. More precisely, this situation is achieved when $J_2 < J_1$ and when η_{ph}/η_{el} varies continuously and crosses 1 from below. As soon as $\eta_{ph} > \eta_{el}$, $\delta(s)$ is surely negative for s large enough. $\Psi_0(\zeta)$ is non-convex in infinitely many open intervals associated with all the rationals r/s with high-order s. Beyond the stability threshold, the width of these intervals grows so that they overlap. Figure 9 shows the difference $\Delta(\zeta) = \Psi_0(\zeta) - \Psi_{env}(\zeta)$ for several values of η_{ph} and all rationals with denominator s smaller than 20. If one looks at the behaviour of a given commensurate phase, it just undergoes the cascade of phase separations into its successive parent phases as described above.

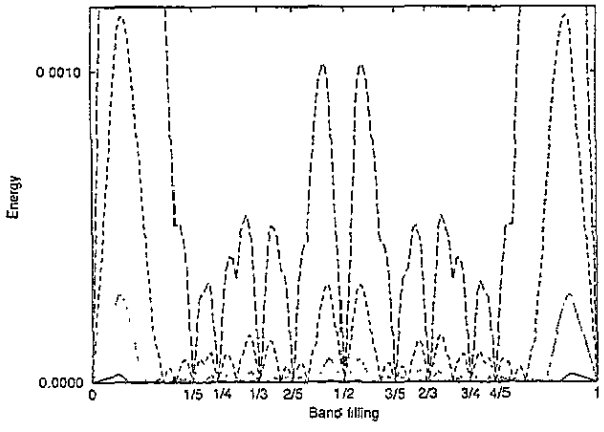

Figure 9. $\Delta(\zeta)$ as a function of the band filling for the toy model ($J_1 = 1$, $J_2 = 0.2$, $\eta_{el} = 0.6$). The curves correspond to the following cases: $\eta_{ph} = 0.70$ (full curve), $\eta_{ph} = 0.75$ (dotted curve), $\eta_{ph} = 0.80$ (broken curve), $\eta_{ph} = 0.85$ (long-dash curve); see example 1 in the text).

For the incommensurate phases, this cascade of phase separations has to be infinite with an accumulation point at $\eta_{ph}/\eta_{el} = 1$. In that situation, the low-order commensurate phases appear to be the most 'robust' phases.

Example 2

$\Psi_0(\zeta)$ may become non-convex in another way. When the model parameters vary beyond the convexity threshold, $\delta(s)$ can first become negative for small $s < S$. This situation is obtained when J_2 increases while $\eta_{ph} < \eta_{el}$. Unlike the previous case, the low-order commensurabilities and their neighbourhood start to be the first unstable phases (see $\Delta(\zeta)$, figure 10).

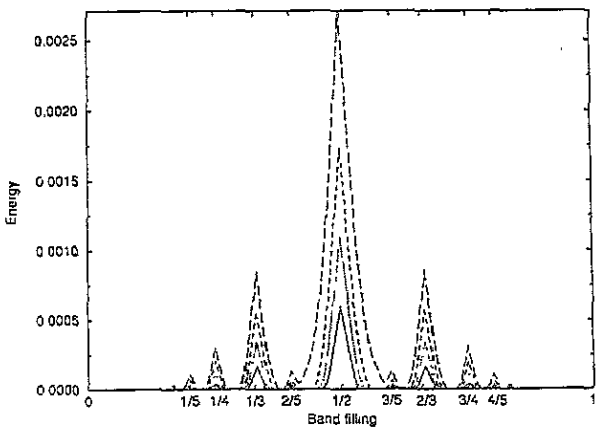

Figure 10. $\Delta(\zeta)$ as a function of the band filling for the toy model ($J_1 = 0.2$, $\eta_{el} = 0.8$, $\eta_{ph} = 0.6$). The curves correspond to the following cases: $J_2 = 0.30$ (full curve), $J_2 = 0.35$ (dotted curve), $J_2 = 0.40$ (broken curve), $J_2 = 0.45$ (long-dash curve); see example 2 in the text.

$\Delta(\zeta)$ is strictly positive in a finite number of open intervals $]\zeta_-, \zeta_+[$ around a few simple rationals ζ_r. The corresponding low-order commensurate phases ζ_r separate into high-order commensurate phases or possibly incommensurate phases with commensurability ζ_- and ζ_+ which both depend continuously as a Devil's staircase on the model parameters.

There are other more complicated situations where, for example, $K(n)$ oscillates at infinity with a non-constant sign. A simpler case is when $K(n)$ alternates its sign for large n. This situation is found in the adiabatic Holstein model at large coupling and when the phonon dispersion is negative ($\gamma < 0$), which yields $\eta_{ph} < 0$. Then, the cascade of phase separations for the incommensurate and commensurate structures should follow different schemes involving, for example, the 'parity' of the rationals r and s or other rules. We did not study all these possible schemes.

We now return to the adiabatic Holstein model with positive dispersion ($\gamma > 0$). When varying γ from zero, we note that the first unstable phases appears in the vicinity of the simple commensurate phase $\zeta = 0$ (and equivalently of the commensurate phase $\zeta = 1$ by the symmetry argument). A non-vanishing stability domain for these commensurate phases is preserved for any values of the parameters (k and γ). The unstable phases correspond to a connected open interval $]0, \zeta_+[$ (and its symmetric one close to 1) where $\Delta(\zeta)$ is strictly positive and $\Psi_0(\zeta)$ is non-convex.

The edge of this interval ζ_+ versus γ apparently varies as a Devil's staircase for small $\zeta_+ \leqslant 3/7$. Until this point, the behaviour of the phase separations can be qualitatively described within the scheme of example 2.

Beyond this point, for larger values of γ, the function $\Delta(\zeta)$ becomes strictly positive in several disconnected intervals which all grow with γ. When they are narrow, these intervals open close to high-order rationals. If we consider any commensurate phase in the interval $]3/7, 1/2[$, we find that it undergoes a cascade of phase separations following (at the beginning) its sequence of commensurate parent phases in a way qualitatively similar to those described in example 1.

These observations show that the discontinuity $\delta(r, s)$ of $\Psi_0'(\zeta)$ at the rational r/s not only depends on s but must also depend on r since the phase separations do not occur simultaneously at all rationals that have the same order. A consequence is that the interaction between the bipolarons cannot be uniquely described by pair interactions as in Hamiltonian (33), because this would imply $\delta(r, s)$ is independent of r. An accurate description of the phase separation necessarily requires a pseudo-spin Hamiltonian (33) with multispin interactions.

6. Concluding remarks

Real quasi-one-dimensional CDW are, in fact, three-dimensional systems containing one-dimensional chains that interact one with another not only through the overlaps between the electronic orbitals of nearest-neighbour chains but also through the elastic coupling between the chains. The transverse overlap is weak by definition, which make the bipolarons very anisotropic. They are rather well localized on single chains, although they could be quite extended along these chains. The bipolaron interaction, which is produced by this interchain overlap, can be neglected at least qualitatively. More important are the interactions due to the dispersion of the phonon branch in the direction transverse to the chains, which have no special reasons to be weak since they participate in the 3D crystal cohesion. These elastic interactions introduce interchain interactions between the bipolarons. Although a precise 3D analysis appears quite difficult, the present study suggests that the phonon dispersion can also induce non-convex forces between the bipolarons and generate complex phase separations in 3D.

For a standard CDW with no phase separation, the Coulomb forces generally play a minor role compared to the electronic driving force which produce the CDW instability†. By contrast, and because they are long-range forces, the Coulomb forces become essential for determining the bipolaronic structure in the event that there would be a phase separation between bipolaronic CDW with different electronic densities, as we will now see.

6.1. Non-$2k_F$ bipolaronic CDW as a consequence of the Coulomb forces on a phase separation

Let us assume that, without Coulomb forces, the CDW exhibits a phase separation between phase A with electronic density ζ_- and phase B with electronic density ζ_+. Whatever the short-range bipolaron interactions are, no phase separation into two macroscopic domains as described above is possible in a real system. Then, the density of Coulomb energy involved in this phase separation would diverge. The electric neutrality of the system forces the density of bipolarons to be uniform at the macroscopic scale and equal to ζ. The divergency of the Coulomb energy can be removed by forming a microstructure which

† When these local interactions are important they must be described at the microscopic level by Hubbard terms in the Hamiltonian. As a result, the nature of the CDW changes and becomes, for example, a spin density wave or a spin Peierls state

alternate domains of phase A and B. This domain superstructure then does not appear as a $2k_F$ CDW.

Even if it is assumed that both the short- and long-range interactions are known, finding precisely the resulting bipolaronic structures is in general quite difficult. However, we can get an intuitive idea of what it could be by a quite phenomenological approach. A simple choice is to assume that the superstructure consists of domain stripes A and B with thickness L_A and L_B. Then, this superstructure involves only one main vector of modulation Q and its harmonics. The length of the unit cell $L = L_A + L_B = 2\pi/|Q|$ of the superstructure along the wave-vector Q is assumed to be a continuous parameter, which means that at this stage we discard any effect of the lattice discreteness or any commensurability effect on Q. The ratio $c = L_A/L_B$ is fixed as $c = (\zeta_+ - \zeta)/(\zeta - \zeta_-)$ in order that the electronic density be ζ.

The contribution to the energy density due to the presence of these interfaces AB and BA depends on their orientation if, as we pointed out, there are local interchain interactions induced by some phonon dispersion. The energy per unit surface for a pair of interfaces AB and BA (supposed to be far apart and non-interacting) is $e_{AB}(\hat{Q})$ and the average interface energy per unit volume is $e_{AB}(\hat{Q})|Q|/2\pi$ where $\hat{Q}$ represents the unit vector parallel to Q.

The Coulomb energy Φ_{Coul} for a 3D charge density $\rho(r)$ with Fourier transform $\rho(q)$ is

$$\Phi_{\text{Coul}} = \int \frac{1}{2\epsilon(q)} \frac{|\rho(q)|^2}{|q|^2} \mathrm{d}q \tag{41}$$

where $\epsilon(q)$ is the dielectric constant of the material at wave-vector q, which we can assume to be independent of q (for small q). The main part of the Coulomb energy of the structure per unit volume is given by its main harmonics and scales as $\kappa/|Q|^2$ where κ is roughly proportional to the square of the charge modulation between the two phases A and B.

The minimum of the total energy

$$\Phi_{\text{tot}} = \frac{\kappa}{|Q|^2} + e_{AB}(\hat{Q}) \frac{|Q|}{2\pi} \tag{42}$$

with respect to Q is obtained for a certain orientation of the wave-vector modulation $\hat{Q}$ and a certain length Q. The orientation of Q is entirely determined by the dispersion curves of the phonons in the direction perpendicular to the chains. *A priori*, it is not necessarily a simple direction of the crystal. The length of the wave-vector modulation is fixed to a non-zero and finite value, because of the Coulomb energy.

If the crossing energy between two interfaces AB and BA is positive, the above solution with a single modulation wave-vector looks appropriate. If this crossing energy is negative, the minimization of the total energy would be better obtained by a microdomain structure which is modulated in two directions with, for example, two symmetric wave-vectors. We do not discuss this more complex situation.

In the regime of strong electron–phonon coupling, the first-order transition between phases A and B becomes very sharp with very different electronic densities (for example, 0 and 1) even for a moderately small phonon dispersion. The interface energy e_{AB} becomes relatively large compared to the Coulomb energy. The phase separation and the resulting structure should appear with relatively large microdomains experimentally observable.

In the opposite case, when the system is close to the borderline of phase separation in parameter space, the phases A and B become almost identical with nearby modulation wave-vectors. The interface energy e_{AB} becomes small compared to the Coulomb parameter

κ. The phase separation should result as small microdomains with a size of a few unit cells with thick interfaces AB and BA comparable with their relative distance. It then becomes not quite appropriate to speak about a phase separation in that case. It is better to say that the bipolaronic structures reordered as a new CDW with a wave-vector which is not $2k_F$, those of the standard Peierls CDW. One could also perhaps better interpret the new CDW as a perturbed Peierls CDW with a superstructure of advanced and delayed discommensurations changing the initial periodicity.

6.2. Are the real CDW bipolaronic?

After almost two decades of intensive study, both experimentally and theoretically, the standard Peierls–Fröhlich theory and its improvements including the role of impurities, still fail to yield a consistent interpretation of the whole set of observed features, in real quasi-one-dimensional CDW. The eminent specialist P Monceau pointed out in the conclusion of his review paper [31]: 'The general properties of these states (CDW) are more or less analysed ... However, in spite of all these efforts *most of the fundamental questions* remain unsolved'.

Beside the fact that the existence of bipolaronic CDW is now well founded on a solid theoretical basis, the bipolaronic theory of CDW is not yet developed enough for practical predictions in real compounds. However, the richness of the new phenomenology, which remains to be explored through a bipolaronic approach of real CDW, should motivate more efforts to find new theories of the real CDW which could be more satisfactory than standard Peierls–Fröhlich theory. We cannot discuss now the whole set of experimental facts observed in most (or all?) real CDW which are in disagreement with standard Peierls–Fröhlich theory and which could support a bipolaronic theory (with an electron–phonon coupling generally in the intermediate regime). We mostly focus here on the specific problem concerning the anomalous value observed for the wave-vector of the CDW in $(TaSe_4)_2I$.

Let us note, however, that although the concept of a bipolaron is easy to define in the limit of large electron–phonon coupling, this concept becomes physically useless. Indeed, in that limit the bipolarons are nothing other than well localized chemical covalent bonds which are strongly pinned to the structure up to the crystal melting temperature. Although in the limit of a very large electron–phonon coupling the phase separation of CDW almost surely occurs, the so-called resulting bipolaron ordering is nothing but the true crystal structure.

The physically interesting systems are those in the intermediate range of electron–phonon coupling, where the bipolarons extend significantly beyond the single sites or bonds and are weakly pinned to the lattice so that we can expect interesting phase transitions by melting of the bipolaron structure (before the whole crystal). This situation does not occur in isotropic 3D systems because, in most cases, the bipolarons are necessarily well localized and pinned to the lattice. There is a first-order transition between a strongly localized bipolaron and the extended (non-localized) electrons. In fact, the bipolaron formation is greatly favoured in quasi-1D systems or, more generally, when the Fermi surface has good nesting properties. In the intermediate coupling regime, the bipolarons can exist while relatively extended and weakly pinned to the lattice. Up to now, no bipolaronic structures have been experimentally recognized because, concerning their structural aspect, they could be easily confused with Peierls–Fröhlich CDW.

In the literature, the observed wave-vector of most CDW at 0 K is generally found to be consistent with the $2k_F$ wave-vector, which can be expected from a knowledge of the band filling. For example, blue bronze has been analysed in detail. We picked from [9] and [36], the values of the parameters (bandwidth, band filling, Peierls gap and phonon dispersion parameter) obtained either from real experiments or from band calculations, which have

to be used in our model to describe this material. The parameters of blue bronze are represented by an asterisk on figure 11. One notices the following two points.

(i) The ratio of the electronic gap (at 0 K) to the bare bandwidth is larger than 0.1, which is the threshold of existence for the Peierls–Fröhlich CDW. As well as most other real CDW where this parameter may be known, blue bronze is well inside the domain of bipolaronic CDW far away from a Peierls–Fröhlich CDW.

(ii) Although close to the borderline, blue bronze is still in the region where there is no phase separation.

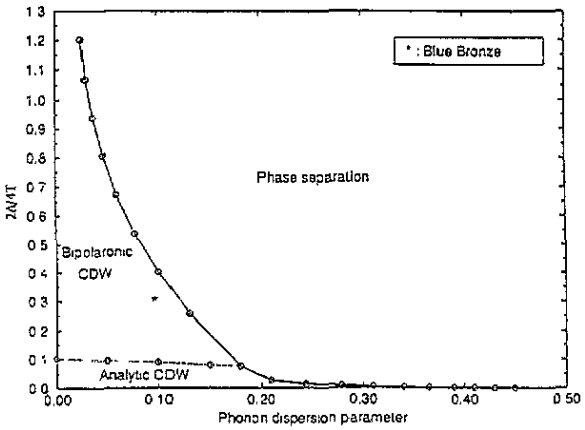

Figure 11. Phase diagram in the $(2\Delta/4T, \gamma)$ plane. We choose the ratio of the Peierls gap 2Δ with the bare bandwidth (which is easier to estimate in real systems) instead of the dimensionless electron–phonon coupling constant k. The parameters of blue bronze are represented by the symbol $*$.

This is in agreement with the fact that the observed $2k_F$ vector of blue bronze agrees with known band filling†. This remark makes it hard to believe that blue bronze is indeed a Peierls–Frölich CDW at 0 K. (Note, however, that a theory for the behaviour of bipolaronic CDW as a function of temperature is missing, for a better understanding of the thermal behaviour of blue bronze and other CDW.)

Up to now, only one system $(TaSe_4)_2I$ [30] is known where the standard interpretation for the observed value of the modulation wave-vector of the CDW poses a serious problem. It is known that there are two free electrons for four Ta atoms per chain in the unit cell. The $2k_F$ CDW should have a period containing four Ta atoms along one chain, which means that $2k_F$ should be equal to c^*. Because of this commensurability, the CDW should appear in diffraction spectra at the spots of forbidden Bragg peaks (space group I422). In addition, this commensurate CDW should be pinned to the lattice and the material should be a strong insulator. In fact, the observed value for the CDW wave-vector is quite different. It is $0.085c^*$ along the chain and there are also unusual transverse components

† Three electrons per cells are supposed to be shared between two almost equivalent electronic bands. The wave-vectors of the two bands lock one with each other at the average wave-vector $3/4b^*$ [33].

$0.05a^*$ and $0.05b^*$†. Lorenzo and co-workers [30] suggested that an antiphase arrangement due to Coulombic repulsion on adjacent chains lead to a CDW wave-vector at $\pm a^* + c^*$ (or $\pm b^* + c^*$), while some attempts of interpretation for the small deviation of the actual CDW wave-vector, symmetry breaking between chains or lattice-mode interactions, have been proposed (see references in [30]). Otherwise, neutron scattering experiments in this compound exhibited neither any significant phonon softening nor any phason mode, but only a quasi-elastic diffusion around the transition point, which supports the idea that this CDW could be bipolaronic [29]. Concerning all the other experiments done, this compound shares the typical properties of the other 1D CDW, for example the non-linear behaviour of charge transport and the glassy behaviour observed through heat transport measurements [32].

If the CDW were commensurate, it could be viewed as an array of equidistant bipolarons in each unit cell. This bipolaronic sequence could be labelled by the periodic coding sequence $\{\cdots 000100010001\cdots\}$ along the chain of tantalum (which contains four atoms per unit cell). The occupied Ta sites are coded by 1 and the unoccupied sites by 0 (they might not be sites but Ta–Ta bonds). We have no estimation of the elastic interactions between the bipolarons which could be mediated by the 3D dispersion of the phonons coupled to the conducting electrons of this material. If we assume that these interactions are large enough, we may find an explanation for the fact that a non-$2k_F$ CDW structure also resulting from the Coulomb forces can appear. Following the above arguments, we should be in an intermediate regime for the electron–phonon coupling, the phase separation of the CDW should not be sharp, i.e. the system is close to the boundary of the domain of phase separation (see figure 11). One can expect that the Coulomb forces will maintain a CDW in a configuration close to the standard $2k_F$ configuration, but with some 'alterations'.

We can make our idea more precise by a simple example (which does not presume about the real bipolaron ordering in the CDW of $(TaSe_4)_2I$). One of the smallest alterations that would change the CDW wave-vector into $c^*/12 = 0.0833c^*$ (close to the real value 0.085) has a unit cell containing 12 unit cells of the underlying crystal coded as {000100010001001000100010001000100010000100010001}. This structure is obtained by a phase shift of the middle part of the supercell structure, which can be viewed as a pair of advanced and delayed discommensurations. It can be also viewed as alternate domains with commensurability 6/23 and 6/25, which makes 1/4 in average. This example suggests that even a small alteration of the bipolaronic CDW is enough to change its wave-vector to the observed value. In addition, it creates discommensurations that are more mobile because their pinning is much weaker than those of the commensurate CDW. These discommensurations make the CDW more 'plastic' and allows it to carry a non-linear electric supercurrent.

The convolution of such a sequence $\{\sigma_i\}$ by a shape factor (13) extended over few unit cells, yields the electronic density $\{\rho_i\}$. A second convolution of the electronic density with the lattice shape factor yields a lattice modulation which can become quite close to a sine function, although the CDW is supposed to be bipolaronic. There are many other possible arrangements of the bipolaronic structure in 3D, including incommensurate structures. In the future it should perhaps be possible to determine experimentally (by very accurate x-ray synchrotron experiments on the whole set of diffraction spots and their harmonics) both these shape factors and the corresponding exact 3D bipolaronic distribution.

† Recent experiments [35] have shown that doping $(TaSe_4)_2I$ with isoelectronic impurities Nb substituted to Ta, induces important variations of the CDW wave-vector. Since the band filling is supposed to be unchanged by doping, this result can be considered as experimental proof that the wave-vector of the CDW of $(TaSe_4)_2I$ is not $2k_F$.

In summary, we have proven on a specific 1D model that the dispersion of the phonon branches involved in the formation of a CDW can induce phase separations at 0 K for the ground state of a $2k_F$ bipolaronic CDW, for a parameter range that is physically reasonable. We have then shown that the Coulomb forces should reconstruct a new bipolaronic CDW, with a wave-vector that could be quite different from $2k_F$. Finally, we suggested that the unexpected wave-vector of the CDW of $(TaSe_4)_2I$ could be explained on the basis of the main idea supported by this paper, i.e. at large or even at moderate electron–phonon coupling the bipolaronic CDW ordering not only results from the $2k_F$ Peierls instability but also on both the elastic and Coulomb forces which could favour another CDW ordering.

Acknowledgments

We thank J E Lorenzo and R Currat for interesting discussions and communicating some of their experimental results prior to publication. We are also indebted to H Moudden for useful discussions concerning CDW. Financial support has been received from the European Network ERBCHRXCT930331.

References

[1] Peierls R E 1955 *Quantum Theory of Solids* (Oxford: Oxford University Press) p 108
[2] Toombs G A 1978 *Phys. Rep.* **40** 181
[3] Aubry S and Quémerais P 1989 *Low-Dimensional Electronic Properties of Molybdenum Bronzes and Oxides* ed C Schlenker (Dordrecht: Kluwer) p 295
[4] Holstein T 1959 *Ann. Phys., NY* **8** 325, 343
[5] Aubry S, Abramovici G and Raimbault J L 1992 *J. Stat. Phys.* **67** 675
[6] Baesens C and MacKay R 1994 *Nonlinearity* **7** 59
[7] Emin D 1980 *The Physics of MOS Insulators* ed G Lucovsky, S T Pantelides and F L Galeener (Oxford: Pergamon) p 39
[8] Alexandrov A S, Ranninger J and Robaszkiewicz S 1986 *Phys. Rev.* B **33** 4526
[9] Noguera C and Pouget J P 1991 *J. Physique* **1** 1035
[10] Quémerais P 1987 *PhD thesis* Université de Nantes
[11] Pouget J P 1989 *Low-Dimensional Electronic Properties of Molybdenum Bronzes and Oxides* (Dordrecht: Kluwer) p 87
[12] Shastry B S 1983 *Phys. Rev. Lett.* **50** 633
[13] Aubry S 1994 *Physica* **71D** 196
[14] MacKay R S 1992 *Physica* **50D** 71
[15] Beni G, Pincus P and Kanamori J 1974 *Phys. Rev.* B **10** 1896
[16] Tsironis G and Aubry S 1995 in preparation
[17] Hubbard J 1978 *Phys. Rev.* B **17** 494
[18] Pokrovsky V I and Uimin G L 1978 *J. Phys. C: Solid State Phys.* **11** 3535
[19] Bak P and Bruinsma R 1982 *Phys. Rev. Lett.* **49** 249
[20] Aubry S 1983 *J. Phys. C: Solid State Phys.* **16** 2497
[21] Aubry S, Gosso J P, Abramovici G, Raimbault J L and Quémerais P 1991 *Physica* **47D** 461
[22] Kuhn C and Aubry S 1994 *J. Phys.: Condens. Matter* **6** 5891
[23] Selke W and Fisher M E 1979 *Phys. Rev.* B **20** 257
[24] Selke W 1988 *Phys. Rep.* **170** 213
[25] Vallet F, Schilling R and Aubry S 1988 *J. Phys. C: Solid State Phys.* **21** 67
[26] Aubry S, Godreche C and Luck J M 1988 *J. Stat. Phys.* **51** 1033
[27] Aubry S 1989 *J. Physique Colloq.* C3 **50** 97
[28] Lang S 1966 *Introduction to Diophantine Approximations* (New York: Addison-Wesley)
[29] Lorenzo J E 1992 *PhD thesis* Grenoble University
[30] Lorenzo J E, Currat R, Monceau P, Hennion B and Levy F 1993 *Phys. Rev.* B **47** 10116

[31] Monceau P 1990 *Application of Statistical and Field Theory Methods to Condensed Matter* ed D Baeriswyl *et al* (New York: Plenum) p 357
[32] Monceau P 1985 *Electronic Properties of Inorganic Quasi One-dimensional Materials* ed P Monceau (Dordrecht: Reidel) p 139
[33] Pouget J P, Noguera C, Moudden A H and Moret R 1985 *J. Physique* **46** 1731
[34] Gruber C, Ueltschi D and Jedrzejewski J 1994 *J. Stat. Phys.* **76** 1
[35] Lorenzo J E, Thurston T, Currat R and Monceau P 1995 in preparation
[36] Pouget J P, Hennion B, Escribe-Filippini C and Sato M 1991 *Phys. Rev.* B **43** 8421